CXCL13 drives spinal astrocyte activation and neuropathic pain via CXCR5

Bao-Chun Jiang, De-Li Cao, Xin Zhang, Zhi-Jun Zhang, Li-Na He, Chun-Hua Li, Wen-Wen Zhang, Xiao-Bo Wu, Temugin Berta, Ru-Rong Ji, and Yong-Jing Gao

Inventory of supplementary materials submitted:

I. Supplemental Methods and References

II. Supplementary Tables (5)

III. Supplementary Figures (15)

Supplemental methods

Animals and surgery

Adult ICR mice (male, 8 weeks) were purchased from Experimental Animal Center of Nantong University. *Cxcr5*$^{-/-}$ mice [B6.129S2 (Cg)-Cxcr5$^{tm1Lipp/J}$, stock number: 006659] were purchased from the Jackson Laboratory and C57BL/6 wild-type mice were used as control. The animals were maintained on a 12:12 light–dark cycle at a room temperature of 22 ± 1 ℃ with free access to food and water. To produce a spinal nerve ligation (SNL), animals were anesthetized with isoflurane and the L6 transverse process was removed to expose the L4 and L5 spinal nerves. The L5 spinal nerve was then isolated and tightly ligated with 6-0 silk thread (1). For sham operations, the L5 spinal nerve was exposed but not ligated.

Human tissues

Human spinal cords (two non-diseased donors: 72-year-old male and 54-year-old male) and DRG (one non-diseased donor: 46-year-old female) were obtained from National Disease Research Interchange (NDRI). Healthy lymph nodes (58-year-old male) were kindly provided by the Department of Pathology of the Affiliated Hospital of Nantong University.

Drugs and administration

Recombinant murine CXCL13 was purchased from PeproTech (Peprotech, Rocky Hills, NJ). miR-186-5p mimic (5′-CAA AGA AUU CUC CUU UUG GGC U-3′), its scrambled negative control (5′-UUC UCC GAA CGU GUC ACG UTT-3′), miR-186-5p inhibitor (5′-AGC CCA AAA GGA GAA UUC UUU G-3′), and its scrambled negative control (5′-CAG UAC UUU UGU GUA GUA CAA-3′) were synthesized by RiboBio (Guangzhou, China). Before cell transfection or intrathecal injection, they were mixed with X-tremeGENE siRNA transfection reagent (Roche, Basel, Switzerland) for in vitro experiments and with Lipofectamine 2000 reagent (Invitrogen, Carlsbad, CA) for in vivo experiments, respectively. MEK inhibitor

PD98059 was purchased from Merck KGaA (Darmstadt, Germany). Astroglial toxin L-α-aminoadipate, microglial inhibitor minocycline, and non-competitive NMDA glutamate receptor antagonist MK801 were purchased from Sigma (St Louis, MO). Intrathecal injection was made with a 30 G needle between the L5 and L6 intervertebral spaces to deliver the reagents to the cerebral spinal fluid (2). To induce chemotherapy-induced pain, paclitaxel (6 mg/kg, Cisen Pharmaceutical Co) was intraperitoneally injected (3). The same volume of saline was used as control.

Lentiviral vectors production and intraspinal injection

Three shRNAs targeting the sequence of mice *Cxcl13* (Gene Bank Accession: NM_018866) or *Cxcr5* (Gene Bank Accession: NM_007551) were designed respectively. An additional scrambled sequence was also designed as a negative control (NC). The recombinant lentivirus containing *Cxcl13* shRNA (LV-*Cxcl13* shRNA), *Cxcr5* shRNA (LV-*Cxcr5* shRNA) or NC shRNA (LV-NC) was packaged using pGCSIL-GFP vector by Shanghai GeneChem. The sequences were shown in Supplementary Table 1. The knockdown effect of the above lentivirus was examined by real-time PCR, Elisa (for CXCL13), and Western blot (for CXCR5) on cultured HEK293 cells. In addition, pre-mmu-miR-186 (Accession: MI0000228) sequence (5′-ACU UUC CAA AGA AUU CUC CUU UUG GGC UUU CUC AUU UUA UUU UAA GCC CUA AGG UGA AUU UUU UGG GAA GU-3′) was inserted into lentiviral vector pGV209 (LV-mmu-mir-186) which regulates expression of pre-miRNAs by H1 promoter.

The intraspinal injection was performed as described previously (4). In brief, animals were anesthetized with pentobarbital sodium (40–50 mg/kg, i.p.) and underwent hemilaminectomy at the L1-L2 vertebral segments. Intraspinal injection was performed unilaterally on the left side. After exposure of the spinal cord, each animal received 2 injections (8×10^5 TU per injection, 0.5 mm apart in rostrocaudal axis, 0.8 mm from the midline, 0.5 mm deep) of lentivirus along the L4-L5 dorsal root entry zone using a glass micropipette (diameter 60 μm). The tip of glass micropipette reached to the depth of lamina II-IV of the spinal cord. The dorsal muscle and skin

were then sutured.

RNA isolation, microarray and bioinformatics analysis

Total RNA was isolated from L5 spinal cord segment at 10 days after SNL or sham operation using the TRIzol reagent (Invitrogen, Carlsbad, CA). There were 2 replicates for either sham or SNL group RNA samples. Each RNA sample was a mixture of mRNAs from 3 mice under the same treatment. Following isolation, RNA was further purified with a NucleoSpin® RNA clean-up kit (Macherey-Nagel, Germany). Concentration and yield of RNA samples were determined by a NanoDrop ND-2000 Spectrophotometer (Thermo Scientific, Waltham, MA). Gene expression profiles of L5 spinal cord were assessed with Agilent SurePrint G3 Mouse GE 8×60K Microarray Kit (G4852A) by CapitalBio Corporation (Beijing, China). Microarray results were scanned by Agilent G2565CA Microarray Scanner, and images were quantified using Agilent's Feature Extraction software (Agilent Technologies, Palo Alto, USA). Quantile normalization of raw data and subsequent data processing was performed using the GeneSpring GX v11.5.1 software package (Agilent Technologies). The conserved miRNA sites of *Cxcl13* were predicted using several online programs, including TargetScan (http://www.targetscan.org/), miRDB (http://mirdb.org/miRDB/), and PicTar (http://pictar.mdc-berlin.de/). The data predicted by TargetScan was shown in Supplemental Table 2. The sequence conservation of miR-186-5p and its binding site in *Cxcl13* 3'-UTR among chimpanzee, rhesus, human, rat, mouse, and pig was analyzed using ClustalW2.

Real-time Quantitative PCR (qPCR) for mRNAs and miRNAs

For mRNA detection, the total RNA of the spinal cord or cultured cells was extracted using Trizol reagent (Invitrogen). One microgram of total RNA was reverse transcribed using an oligo(dT) primer according to the manufacturer’s protocol (Takara, Shiga, Japan). For miRNA detection, small RNAs were extracted using RNAiso kit (Takara), and 10 ng of small RNA were reversely transcribed into cDNA using the One Step PrimeScript miRNA cDNA Synthesis Kit (Takara) according to

manufacturer's instructions. qPCR analysis was performed in the Real-time Detection System (Rotor-Gene 6000, Hamburg, Germany) by SYBR green I dye detection (Takara). The detailed primer sequences for each gene were listed in Supplementary Tables 3 and 4. The PCR amplifications were performed at 95 ℃ for 30 s, followed by 40 cycles of thermal cycling at 95 ℃ for 5 s and 60 ℃ for 45 s. GAPDH and U6 small nuclear RNA were used as endogenous control to normalize differences for mRNA and miRNA detection, respectively. Melt curves were performed on completion of the cycles to ensure that nonspecific products were absent. Quantification was performed by normalizing Ct (cycle threshold) values with GAPDH Ct (mRNA) or U6 Ct (miRNA) and analyzed with the $2^{-\Delta\Delta CT}$ method.

Semi-Quantitative reverse transcription PCR (RT-PCR)

After RNA extraction and cDNA reverse transcription, 2 μl of cDNA samples were amplified. PCR reaction mixtures were heated to 95˚C for 3 min, and then subjected to an appropriate amount of cycles of 95˚C for 30 sec, 60˚C for 30s, and 72˚C for 1 min, with a final incubation at 72˚C for 7 min. After that, PCR products (10 μl) were electrophoresed on 3% agarose gel with DL500 DNA Marker (TaKaRa). The agarose gels were stained with DuRed (Biotium) and visualized under UV light.

DNA extraction and genotyping

About 3 mm of the mouse tails were cut from C57BL/6 wild-type and *Cxcr5*$^{-/-}$ mice, and then used to extract DNA with the phenol-chloroform method. PCR was performed using the primer sets and genotyping protocol described below from the Jackson Laboratory. Primers included common forward primer oIMR7120: 5′-CGG AGA TTC CCC TAC AGG AC-3′, wild type reverse primer oIMR7121: 5′-GAT CTT GTG CAG AGC GAT CA-3′, mutant reverse primer oIMR8963: 5′-AAT TCG CCA ATG ACA AGA CG-3′. For PCR amplification, approximately 500 ng DNA was used in a 50 μL reaction volume containing 25 μl 2×Taq PCR MasterMix (Tiangen Biotech), 1 μM primers of oIMR7120, oIMR7121, or oIMR8963. Reactions initially were denatured at 94 ℃ for 3 minutes followed by 35 cycles at 94 ℃ for 30

seconds, 60 ℃ for 30 seconds, 72 ℃ for 30 seconds and a final extension at 72 ℃ for 2 minutes. Amplicons were separated using 1.5% agarose gel, stained with DuRed (Biotium) and photographed with GelDoc-It Imaging System (UVP).

Construction of vectors

The partial 3′-UTR sequences of *Cxcl13* that contain the miR-186-5p, miR-1264-3p, miR-325-3p target region were respectively cloned into pmirGLO dual-luciferase reporter vector (Promega, Madison, WI) by creating the artificial SacI/XbaI sticky ends using oligonucleotide annealing. The pmiR-GLO luciferase vectors containing the mutant miR-186-5p, miR-1264-3p, or miR-325-3p binding site were also constructed using the mutated oligonucleotide pairs (Supplementary Table 5). All the constructs were sequenced to prove sequence integrity.

Dual-luciferase reporter assays

Activities of firefly and Renilla luciferase were measured using the Dual-Glo Luciferases Assay System (Promega, Madison, WI). HEK293 cells were seeded in 6-well plates. 1000 ng/ml firefly luciferase vector accompanied by 50 ng/ml control Renilla luciferase vector, and microRNA mimics (30 or 150 nM) or scrambled negative control were co-transfected using the Xtreme GENE siRNA Transfection Reagent (Roche). Luciferase assays were performed 24 h after transfection.

Spinal dorsal horn neurons culture

Primary cultures of spinal cord dorsal horn neurons were prepared from neonate ICR mice (P3) using a procedure modified from a previously described method (5). Briefly, after decapitation, a laminectomy was performed and the spinal cord was carefully removed. Superficial dorsal horn was isolated and cut into several strips which were then incubated for 45 min at 37 ℃ in Hanks' balanced salt solution (HBSS, Invitrogen) containing papain (15 U/ml, Worthington Biochemical, Lakewood, NJ), rinsed 3 times with HBSS, and placed in culture medium containing Neurobasal (Invitrogen), 5% fetal bovine serum (FBS, Invitrogen), heat-inactivated horse serum (5%,

Invitrogen), L-glutamax-1 (2 mM, Invitrogen), and B-27 (1%, Invitrogen), penicillin (100 U/ml, Invitrogen) and streptomycin (100 μg/ml, Invitrogen). The fragments were mechanically dissociated by gently triturating with a fire-polished pasteur pipette. The resulting cell suspension was plated onto 13-mm poly-D-lysine- and collagen-coated coverslips, and cultured for 5 to 7 days in humidified air with 5% CO_2 at 37 ℃.

Astrocyte culture

Primary astrocytes cultures were prepared from the cerebral cortexes of neonatal C57BL/6 or *Cxcr5*$^{-/-}$ mice (P2) (6). The cerebral hemispheres were isolated and transferred to ice-cold Hank's buffer and the meninges were carefully removed. Tissues were then minced into ~1 mm pieces, triturated, filtered through a 60 μm nylon screen, and collected by centrifugation at ~3000 g for 5 min. The cell pellets were dispersed with a pipette and resuspended in a medium containing 10% FBS in low glucose DMEM (Dulbecco's Modified Eagle's Medium). After trituration, the cells were filtered through a 10 μm screen and then plated into 6-well plates at a density of 2.5×10^5 cells/cm^2, and cultured for about 10 days. The medium was replaced twice a week with 10% FBS. Dibutyryl cAMP (0.15 mM, Sigma-Aldrich) was added to induce differentiation when the cells were grown to 95% confluence. Prior to transfection or stimulation, reduced serum medium (Opti-MEM, Invitrogen) was replaced. Astrocytes were incubated for different time periods ranging from 1 h to 3 h depending on the experiment. After the treatment, the astrocytes were collected for Western blot.

For astrocytes injection, astrocytes from C57BL/6 or *Cxcr5*$^{-/-}$ mice were treated with CXCL13 (100 ng/ml) for 3 h (7). Astrocytes were washed with 0.01 M PBS for three times, centrifuged for 5 min at 3,000 g, and resuspended in PBS. About $2\sim4 \times 10^4$ astrocytes in 10 μl PBS were injected intrathecally.

ELISA

CXCL13 ELISA kit for mouse or human was purchased from R&D systems. Animals were transcardially perfused with PBS. The L5 spinal cord, lymph node, and spleen

were dissected. The cerebral spinal fluid（CSF）was collected from cisterna magna. The tissues and cell lysates were homogenized in a lysis buffer containing protease and phosphatase inhibitors (Sigma). Protein concentrations were determined by BCA Protein Assay (Pierce, Rockford, IL). For each reaction in a 96-well plate, 100 μg of protein (or 10 μl CSF) was used, and ELISA was performed according to manufacturer's protocol. The standard curve was included in each experiment.

Western blot

Protein samples were prepared in the same way as for ELISA analysis. Protein samples (30 μg) were separated on SDS–PAGE gel and transferred to nitrocellulose blots. The blots were blocked with 5% milk and incubated overnight at 4℃ with antibody against CXCR5 (rabbit, 1:100, Santa Cruz, sc-30029), pERK (rabbit, 1:500, Cell Signaling, 9101, Beverly, MA), ERK (rabbit, 1:500, Cell Signaling, 9102), and GAPDH (mouse, 1:20000, Millipore, MAB374, Billerica, MA). These blots were further incubated with HRP-conjugated secondary antibody, developed in ECL solution, and exposed onto Hyperfilm (Millipore) for 1–5 min. Specific bands were evaluated by apparent molecular size. The intensity of the selected bands was analyzed using Image J software (NIH, Bethesda, MD).

Immunohistochemistry and immunocytochemistry

Animals were deeply anesthetized with isoflurane and perfused through the ascending aorta with PBS followed by 4% paraformaldehyde with 1.5% picric acid in 0.16 M PB. After the perfusion, the L5 spinal cord segment or spleen was removed and postfixed in the same fixative overnight. Spinal cord or spleen sections (30 μm, free-floating) were cut in a cryostat and processed for immunofluorescence as we described previously (6). The sections were first blocked with 5% goat serum for 2 h at room temperature, then incubated overnight at 4℃ with the following primary antibodies: CXCL13 (goat, 1:100, Santa Cruz, sc-8182) or CXCR5 (rabbit, 1:100; Santa Cruz, sc-30029), glial fibrillary acidic protein (GFAP, mouse, 1:5000, Millipore, MAB360), NeuN (mouse, 1:1000, Millipore, MAB377), IBA-1 (rabbit, 1:3000, Wako,

019-19741, Tokyo, Japan), OX-42 (mouse, 1:100, AbD Serotec, MAC275GA), and pERK (rabbit, 1:500, Millipore, 9101). The sections were then incubated for 1 h at room temperature with Cy3- or FITC-conjugated secondary antibodies (1:400, Jackson ImmunoResearch, West Grove, PA). For double immunofluorescence, sections were incubated with a mixture of mouse and rabbit primary antibodies followed by a mixture of FITC- and Cy3-conjugated secondary antibodies. The specificity of CXCL13 primary antibody was tested by preabsorption experiment. Spinal cord or spleen sections were incubated with a mixture of CXCL13 primary antibody and the corresponding blocking peptide for CXCL13 (25 μg/ml; Santa Cruz) overnight, followed by secondary antibody incubation. The stained sections were examined with a Leica fluorescence microscope, and images were captured with a CCD Spot camera.

For immunocytochemistry, cultured dorsal horn neurons were fixed with 4% paraformaldehyde for 20 minutes, and processed for immunofluorescence with CXCL13 (goat, 1:200; Santa Cruz, sc-8182) and MAP2 (mouse, 1:5000; Sigma-Aldrich, M1406) antibody as shown above.

In situ hybridization (ISH) of *Cxcl13* mRNA and miR-186-5p

Cellular localization of *Cxcl13* was performed using the mouse *Cxcl13* mRNA ISH Assay Kit (Boster Bio-Tech, Wuhan, China) as described previously (4). Briefly, in situ hybridizations were performed in 14 μm cryosections from spinal cord. Sections were fixed in 4% paraformaldehyde/0.1 M PBS for 30 min followed by washes in DEPC-treated ultrapure water. After treatment with a mixture of 30% H_2O_2 and methanol (v/v=1:50) for 30 minutes, sections were treated with proteinase K (Boster) for 2 min at room temperature. Prehybridization procedures were performed under RNase-free conditions for 4 h at room temperature. Hybridization was carried out with hybridization probe specific to *Cxcl13* at 42 ℃ overnight in hybridization buffer. Sections were then incubated in blocking solution at 37 ℃ for 30 min and in mouse-anti-DIG-biotin for 60 min, washed, incubated using SABC-FITC regent (Boster) for 30 min.

Locked nucleic acid-based in situ detection of miR-186-5p was performed as described previously (8). Except for prehybridization and hybridization, the ISH procedures of miR-186-5p were the same as that of *Cxcl13* mRNA. In brief, sections were prehybridized in hybridization solution (50% deionised formamide, 0.3 M NaCl, 5 mM EDTA, 10 mM $NaPO_4$, 0.5 mg/ml yeast tRNA, 10% Dextran Sulfate, 1×Denhardt's solution) at 25° C below the predicted Tm value of the LNA probe for 2 h. Next, sections were incubated with 5′-DIG and 3′-DIG labeled mature miR-186-5p miRCURY LNA™ detection probe (/5DigN/AGC CCA AAA GGA GAA TTC TTT G/3Dig_N/) or microRNA Detection Control Probe for ISH (/5DigN/GTG TAA CAC GTC TAT ACG CCC A/3Dig_N/) (Exiqon, Vedbæk, Denmark) at 53 ℃ overnight.

To identify the cell types expressing *Cxcl13* and miR-186-5p, the above sections under ISH were incubated overnight at 4 ℃ with primary antibodies against GFAP (mouse, 1:6000, Millipore, MAB360), NeuN (mouse, 1:1000, Millipore, MAB377), IBA-1 (rabbit, 1:3000, Wako, 019-19741), or CXCL13 (goat, 1:50, Santa Cruz, sc-8182). On the following day, Cy3-conjugated secondary antibody was added and incubated for 2 h. The signal was detected with a Leica SP8 Gated STED confocal microscope (Leica Microsystems, Wetzlar, Germany).

Behavioral analysis

Animals were habituated to the testing environment daily for at least 2 days before baseline testing. All the behavioral experimenters were done by individuals that were blinded to the treatment or genotypes of the mice.

Hargreaves test. The animals were put in a plastic box placed on a glass plate, and the plantar surface was exposed to a beam of radiant heat through a transparent glass surface (IITC model 390 Analgesia Meter; Life Science, Woodland Hills, CA). The baseline latencies were adjusted to 12 to 15 seconds with a maximum of 20 seconds as cutoff to prevent potential injury. The latencies were averaged over 3 trials, separated by a 5-minute interval (9).

Von Frey test. The animals were put in boxes on an elevated metal mesh floor and allowed 30 min for habituation before examination. The plantar surface of the

hindpaw was stimulated with a series of von Frey hairs with logarithmically incrementing stiffness (0.02-2.56 grams, Stoelting, Wood Dale, IL), presented perpendicular to the plantar surface (2-3 seconds for each hair). The 50% paw withdrawal threshold was determined using Dixon's up-down method (10).

Tail immersion test. The temperature of the water was set at 48, 50 or 52℃. The tail flick latency was recorded. The cutoff was set at 10 seconds to avoid potential injury (11).

Rota-rod test. Mice were trained on the rota-rod for 3 min at a speed of 10 rpm, till the mice no longer fell off it. For testing, the speed was set at 10 rpm for 60 s and subsequently accelerated to 80 rpm in 5 minute. The time taken for mice to fall after the beginning of the acceleration was recorded (12).

Locomotor activity test. The sedative property of the lentiviral vectors, miR-186 mimic, and inhibitor was investigated by recording spontaneous locomotor activity of mice in an open field (13). The animals were placed in the center of an open field of 50 × 50 cm. The locomotor activity was recorded by a webcam and analyzed by ANY-maze software (Stoelting). The total locomotor activity was defined as the travel distance of an animal in 30 min.

Quantification and statistics

All data were expressed as mean ± SEM. The behavioral data were analyzed by two-way repeated measures ANOVA followed by Bonferroni test as the post-hoc multiple comparison analysis. For the analysis of GFAP- or IBA-1-immunoreactivity, the images of the dorsal horn were captured and a numerical value of the intensity was calculated with a computer-assisted imaging analysis system (Image J) (14). The intensity of the background was subtracted in each section. For western blot, the density of specific bands was measured with Image J. CXCR5 levels were normalized to GAPDH and pERK levels were normalized to total ERK (15). Differences between groups were compared using one-way ANOVA followed by Bonferroni test or using Student's *t*-test if only 2 groups were applied. The criterion for statistical significance was $P < 0.05$.

Study approval

All animal procedures performed in this study were reviewed and approved by the Animal Care and Use Committee of Nantong University and were conducted in accordance with the guidelines of the International Association for the Study of Pain.

Supplementary references

1. Kim, S.H., and Chung, J.M. 1992. An experimental model for peripheral neuropathy produced by segmental spinal nerve ligation in the rat. *Pain* 50:355-363.
2. Hylden, J.L., and Wilcox, G.L. 1980. Intrathecal morphine in mice: a new technique. *Eur J Pharmacol* 67:313-316.
3. Liu, X.J., Zhang, Y., Liu, T., Xu, Z.Z., Park, C.K., Berta, T., Jiang, D., and Ji, R.R. 2014. Nociceptive neurons regulate innate and adaptive immunity and neuropathic pain through MyD88 adapter. *Cell Res* 24:1374-1377.
4. Zhang, Z.J., Cao, D.L., Zhang, X., Ji, R.R., and Gao, Y.J. 2013. Chemokine contribution to neuropathic pain: respective induction of CXCL1 and CXCR2 in spinal cord astrocytes and neurons. *Pain* 154:2185-2197.
5. Hugel, S., and Schlichter, R. 2000. Presynaptic P2X receptors facilitate inhibitory GABAergic transmission between cultured rat spinal cord dorsal horn neurons. *J Neurosci* 20:2121-2130.
6. Gao, Y.J., Zhang, L., Samad, O.A., Suter, M.R., Yasuhiko, K., Xu, Z.Z., Park, J.Y., Lind, A.L., Ma, Q., and Ji, R.R. 2009. JNK-induced MCP-1 production in spinal cord astrocytes contributes to central sensitization and neuropathic pain. *J Neurosci* 29:4096-4108.
7. Gao, Y.J., Zhang, L., and Ji, R.R. 2010. Spinal injection of TNF-alpha-activated astrocytes produces persistent pain symptom mechanical allodynia by releasing monocyte chemoattractant protein-1. *Glia* 58:1871-1880.
8. Li, H., Yin, C., Zhang, B., Sun, Y., Shi, L., Liu, N., Liang, S., Lu, S., Liu, Y., Zhang, J., et al. 2013. PTTG1 promotes migration and invasion of human non-small cell lung cancer cells and is modulated by miR-186. *Carcinogenesis* 34:2145-2155.
9. Hargreaves, K., Dubner, R., Brown, F., Flores, C., and Joris, J. 1988. A new and sensitive method for measuring thermal nociception in cutaneous hyperalgesia. *Pain* 32:77-88.
10. Dixon, W.J. 1980. Efficient analysis of experimental observations. *Annu Rev Pharmacol Toxicol* 20:441-462.
11. Ramabadran, K., Bansinath, M., Turndorf, H., and Puig, M.M. 1989. Tail immersion test for the evaluation of a nociceptive reaction in mice. Methodological considerations. *J Pharmacol Methods* 21:21-31.
12. Abbadie, C., Lindia, J.A., Cumiskey, A.M., Peterson, L.B., Mudgett, J.S., Bayne, E.K., DeMartino, J.A., MacIntyre, D.E., and Forrest, M.J. 2003. Impaired neuropathic pain responses in mice lacking the chemokine receptor CCR2. *Proceedings of the National Academy of Sciences* 100:7947-7952.
13. Trevisan, G., Rossato, M.F., Walker, C.I., Oliveira, S.M., Rosa, F., Tonello, R., Silva, C.R., Machado, P., Boligon, A.A., Martins, M.A., et al. 2013. A novel, potent, oral active and safe antinociceptive pyrazole targeting kappa opioid receptors. *Neuropharmacology* 73:261-273.
14. Zhuang, Z.Y., Wen, Y.R., Zhang, D.R., Borsello, T., Bonny, C., Strichartz, G.R., Decosterd, I., and Ji, R.R. 2006. A peptide c-Jun N-terminal kinase (JNK) inhibitor blocks mechanical allodynia after spinal nerve ligation: respective roles of JNK activation in primary sensory neurons and spinal astrocytes for neuropathic pain development and maintenance. *J Neurosci* 26:3551-3560.
15. Miyoshi, K., Obata, K., Kondo, T., Okamura, H., and Noguchi, K. 2008. Interleukin-18-mediated

microglia/astrocyte interaction in the spinal cord enhances neuropathic pain processing after nerve injury. *J Neurosci* 28:12775-12787.

Supplementary Table 1. Target sequences of the shRNAs

Sequence name	Sequence	Size
Cxcl13 shRNA-1	5'-CAA ATG GTT ACA AAG ATT A-3'	22 bp
Cxcl13 shRNA-2	5'-TCG TGC CAA ATG GTT ACA A-3'	22 bp
Cxcl13 shRNA-3	5'- AAA CAT CAT AGA TCG GAT T-3'	22 bp
Cxcr5 shRNA-1	5'-CTG GCC TTC TAC AGT AAC A-3'	22 bp
Cxcr5 shRNA-2	5'-GCT GGC CTG TAT AGC TGT A-3'	22 bp
Cxcr5 shRNA-3	5'-CCA TCA CCT TGT GTG AAT T -3'	22 bp
scrambled shRNA (NC)	5'-TTC TCC GAA CGT GTC ACG T-3'	19 bp

Supplementary Table 2. Conserved mammalian microRNA regulatory target sites for 3 conserved microRNA families in the 3'-UTR regions of *Cxcl13* predicted by TargetScanMouse 6.2

Predicted microRNAs	Binding position of microRNAs	Predicted consequential pairing of target region (top) and miRNA (bottom)	Seed match	Context+ score percentile	Conserved branch length
mmu-miR-1264-3p	Position 572-579 of *Cxcl13* 3'-UTR	5'-AAAGGUUGCUUGUAUAAGAUUUA-3' 3'-UGUCCACGAGUUUAUUCUAAAC-5'	8 mer	97	0.732
mmu-miR-186-5p	Position 725-732 of *Cxcl13* 3'-UTR	5'-AGCCUCUUGUAUCAGAUUCUUUA-3' 3'-UCGGGUUUUCCUCUUAAGAAAC-5'	8 mer	94	1.266
mmu-miR-325	Position 758-765 of *Cxcl13* 3'-UTR	5'-UUCAUCUGGUGUCAUUCAAUAAA-3' 3'-AACUAUCCUCCACGAGUUAUUU-5'	8 mer	94	1.922

Supplementary Table 3. Primer sets used in qPCR for mouse samples

Gene Name	Primer Sequence	Size
Cxcl13	5'-GGC CAC GGT ATT CTG GAA GC-3' 5'-ACC GAC AAC AGT TGA AAT CAC TC-3'	75 bp
Ccl7	5'-CCA CAT GCT GCT ATG TCA AGA-3' 5'-ACA CCG ACT ACT GGT GAT CCT-3'	80 bp
Ccl2	5'-GCA TCC ACG TGT TGG CTC A-3' 5'-CTC CAG CCT ACT CAT TGG GAT CA-3'	95 bp
Cxcl1	5'-GCT TGA AGG TGT TGC CCT CAG-3' 5'-AGA AGC CAG CGT TCA CCA GAC-3'	201 bp
Cxcr5	5'-TGG CCT TCT ACA GTA ACA GCA-3' 5'-GCA TGA ATA CCG CCT TAA AGG AC-3'	102 bp
Gapdh	5'-AAA TGG TGA AGG TCG GTG TGA AC-3' 5'-CAA CAA TCT CCA CTT TGC CAC TG-3'	90 bp
Gfap	5'-CCA AGA TGA AAC CAA CCT GA-3' 5'-TCC AGC GAT TCA ACC TTT C-3'	117 bp
Iba1	5'-ATG AGC CAA AGC AGG GAT T-3' 5'-CTT CAA GTT TGG ACG GCA G-3'	145 bp
β-actin	5'-CAT CCG TAA AGA CCT CTA TGC CAA C-3' 5'-ATG GAG CCA CCG ATC CAC A-3'	171 bp
mir-186-5p	5'-CAA AGA ATT CTC CTT TTG GGC T-3'	
mir-1264-3p	5'-CAA ATC TTA TTT GAG CAC CTG T-3'	
mir-325-3p	5'-TTT ATT GAG CAC CTC CTA TCA A-3'	
U6	5'-GCT TCG GCA GCA CAT ATA CTA A-3' 5'-CGA ATT TGC GTG TCA TCC TT-3'	82 bp

Supplementary Table 4. Primer sets used in RT-PCR for human tissues

Gene	Primer Sequence	Size
Cxcl13	5'-GCT TGA GGT GTA GAT GTG TCC-3' 5'-CCC ACG GGG CAA GAT TTG AA-3'	83 bp
Cxcr5	5'-CAC GTT GCA CCT TCT CCC AA-3' 5'-GGA ATC CCG CCA CAT GGT AG-3'	84 bp
Gapdh	5'-AGC CAC ATC GCT CAG ACA C-3' 5'-GCC CAA TAC GAC CAA ATC C-3'	66 bp

Supplementary Table 5. Oligonucleotide sequences cloned into the pmirGLO vector

Oligonucleotide name	Oligonucleotide sequences
miR-186-5p sense	5'-CTA GCG GCC GCA GCC TCT TGT ATC AGA TTC TTT AT-3'
miR-186-5p antisense	5'-CTA GAT AAA GAA TCT GAT ACA AGA GGC TGC GGC CGC TAG AGC T-3'
Mutated miR-186-5p sense	5'-CTA GCG GCC GCA GCC TCT TGT ATC AGT CGT GAT AT-3'
Mutated miR-186-5p antisense	5'-CTA GAT ATC ACG ACT GAT ACA AGA GGC TGC GGC CGC TAG AGC T-3'
miR-1264-3p sense	5'-CTA GCG GCC GCA AAG GTT GCT TGT ATA AGA TTT AT-3'
miR-1264-3p antisense	5'-CTA GAT AAA TCT TAT ACA AGC AAC CTT TGC GGC CGC TAG AGC T-3'
Mutated miR-1264-3p sense	5'-CTA GCG GCC GCA AAG GTT GCT TGT ATA TCG AAT AT-3'
Mutated miR-1264-3p antisense	5'-CTA GAT ATT CGA TAT ACA AGC AAC CTT TGC GGC CGC TAG AGC T-3'
miR-325-3p sense	5'-CTA GCG GCC GCT TCA TCT GGT GTC ATT CAA TAA AT-3'
miR-325-3p antisense	5'-CTA GAT TTA TTG AAT GAC ACC AGA TGA AGC GGC CGC TAG AGC T-3'
Mutated miR-325-3p sense	5'-CTA GCG GCC GCT TCA TCT GGT GTC ATA GTT ATA AT-3'
Mutated miR-325-3p antisense	5'-CTA GAT TAT AAC TAT GAC ACC AGA TGA AGC GGC CGC TAG AGC T-3'

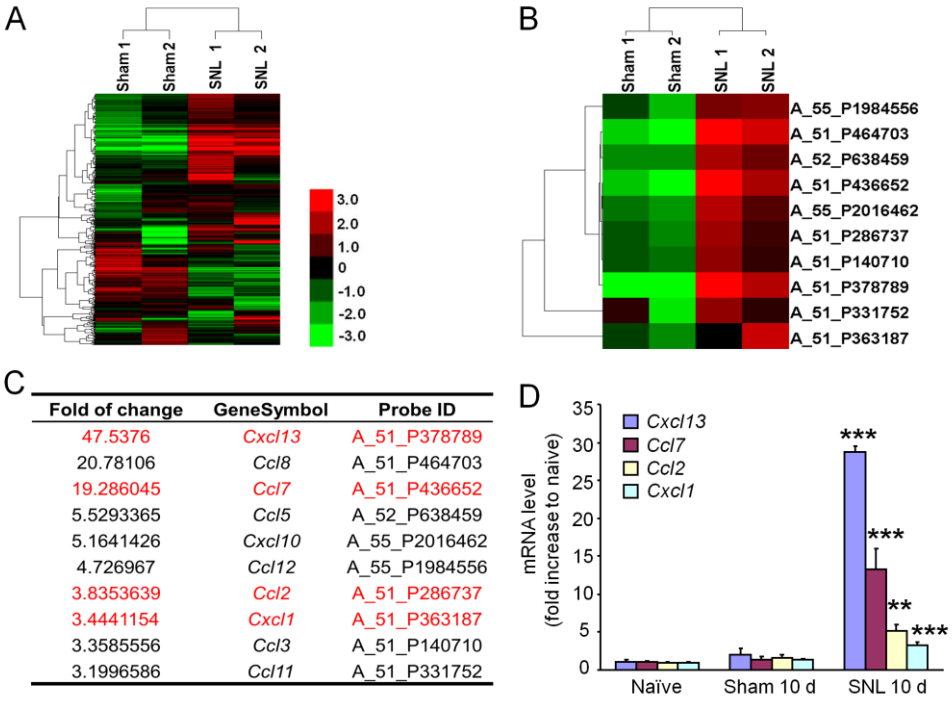

Fold of change	GeneSymbol	Probe ID
47.5376	*Cxcl13*	A_51_P378789
20.78106	*Ccl8*	A_51_P464703
19.286045	*Ccl7*	A_51_P436652
5.5293365	*Ccl5*	A_52_P638459
5.1641426	*Cxcl10*	A_55_P2016462
4.726967	*Ccl12*	A_55_P1984556
3.8353639	*Ccl2*	A_51_P286737
3.4441154	*Cxcl1*	A_51_P363187
3.3585556	*Ccl3*	A_51_P140710
3.1996586	*Ccl11*	A_51_P331752

Supplementary Figure 1. The mRNA expression levels of chemokines are upregulated in the spinal cord 10 days after SNL. (A) Cluster heatmap shows the mRNA expression of 39430 genes in L5 spinal cord of SNL and sham-operated mice. The levels of mRNA expression are represented on a logarithmic scale; red corresponds to high expression and green to low expression. Color scale is shown in the bottom-right corner. (B) Cluster heatmap shows the top 10 chemokine genes that are upregulated in SNL group compared to sham-operated group. (C) Fold change of the up-regulated chemokine genes in the spinal cord after SNL. Notably, *Cxcl13* mRNA level is increased 47-fold after SNL compared to sham-operated mice. (D) Quantitative RT-PCR shows the mRNA expression level of *Cxcl13*, *ccl7*, *ccl2*, *and cxcl1* in the spinal cord. **P < 0.01, ***P < 0.001, SNL vs sham. Student's *t*-test. n=3-6 mice/group.

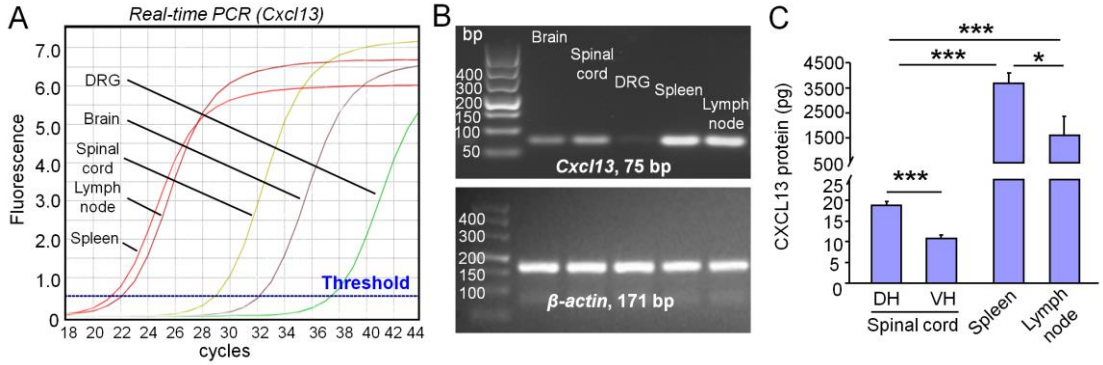

Supplementary Figure 2. CXCL13 expression profile in central nervous system, spleen, and lymph node. (A) Real-time PCR analysis of *Cxcl13* in the brain, spinal cord, DRG, spleen, and lymph node. (B) PCR shows *Cxcl13* expression after 31 cycles of amplification. (C) ELISA results show CXCL13 expression in spinal dorsal horn (DH), spinal ventral horn (VH), spleen, and lymph node in naïve mice. * $P < 0.05$, *** $P < 0.001$. Student's *t*-test. n=4-5 mice/group.

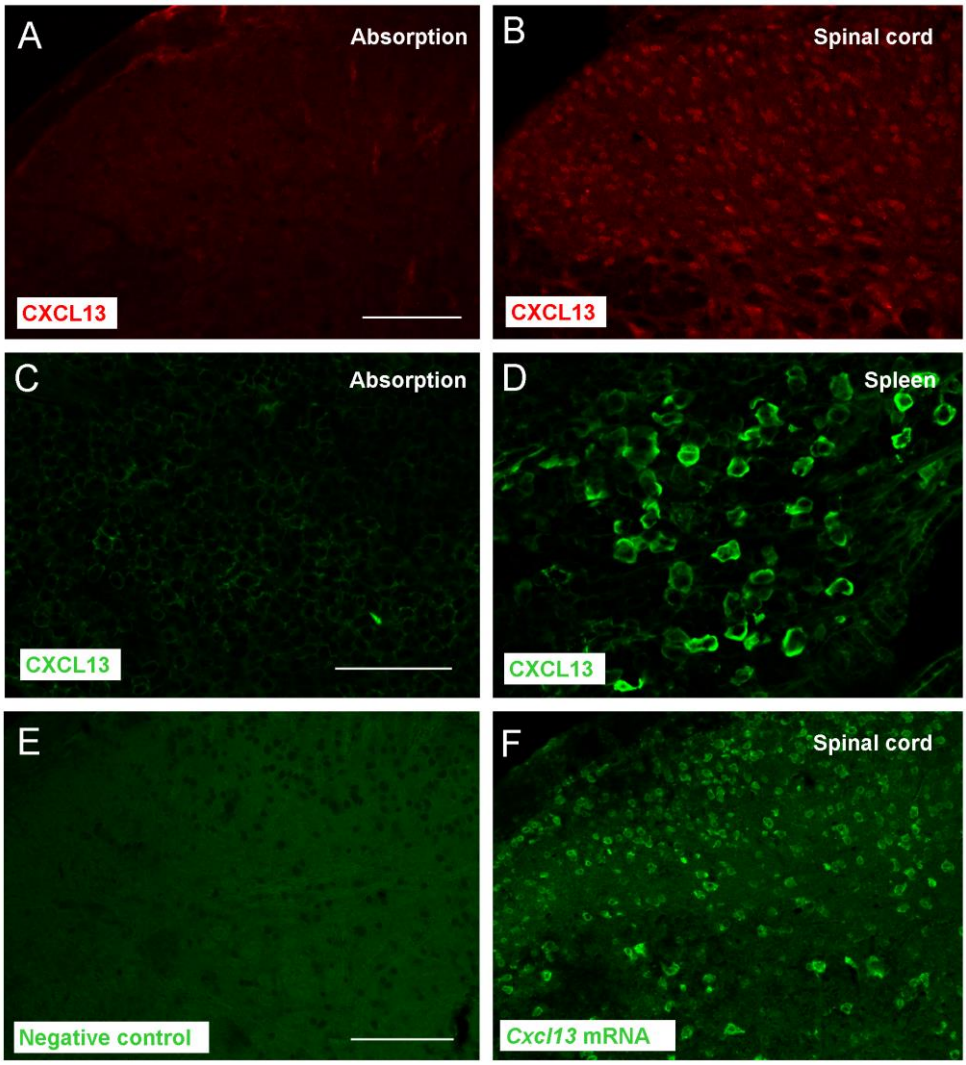

Supplementary Figure 3. Characterization of the specificity of the CXCL13 antibody and the DIG-labelled RNA antisense probe for *Cxcl13*. (A) Pre-absorption of CXCL13 antibody with the CXCL13 blocking peptide abolished the immunostaining in the spinal cord. (B) Immunostaining with CXCL13 antibody in the spinal cord. (C) Pre-absorption of CXCL13 antibody with the CXCL13 blocking peptide abolished the immunostaining in the spleen. (D) Immunostaining with CXCL13 antibody in the spleen. (E) Spinal cord sections were incubated with scrambled negative control probe. (F) Spinal cord sections were incubated with purified *Cxcl13* antisense probes. Scale bar, 100 μm.

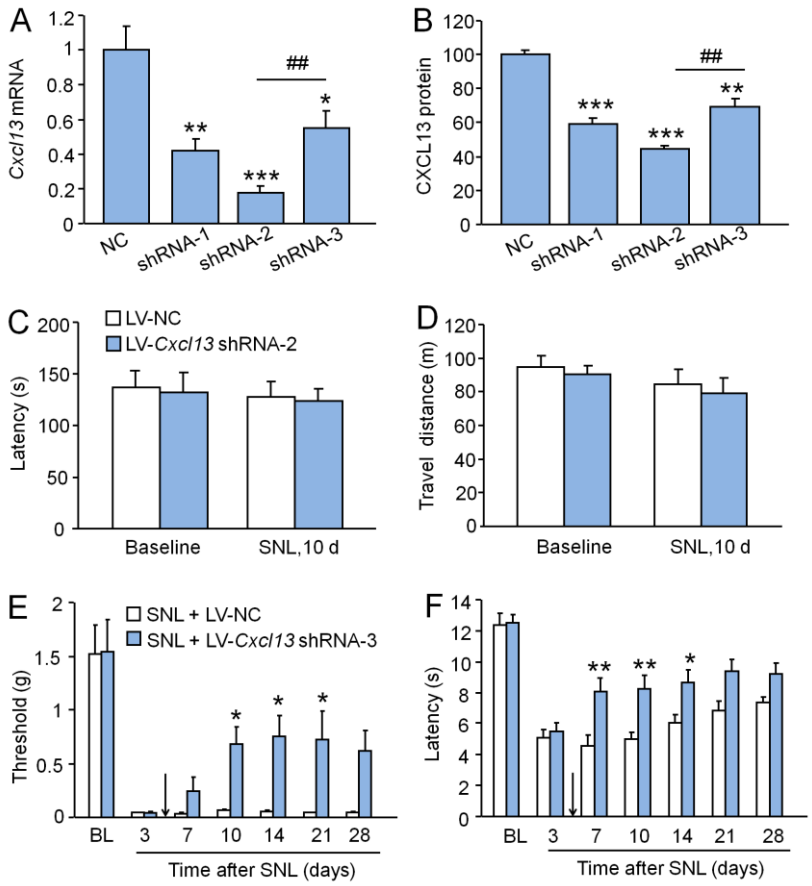

Supplementary Figure 4. Characterization of the knockdown and anti-nociceptive effects of different *Cxcl13* shRNA. (A) Real-time PCR assay of *Cxcl13* shows that all the three shRNAs reduced the *Cxcl13* expression, and shRNA-2 shows the best knockdown effect. * $P < 0.05$, ** $P < 0.01$, *** $P < 0.001$, compared with NC. ## $P < 0.05$. Student's *t*-test. n= 6 for each treatment. (B) ELISA shows CXCL13 protein expression after treatment with shRNAs. ** $P < 0.01$, *** $P < 0.001$, compared with NC. ## $P < 0.01$. Student's *t*-test. n= 3 for each treatment. (C) Rotarod test shows that intraspinal injection of LV-*Cxcl13* shRNA-2 did not affect motor function of the animals. n=7 mice/group. (D) Open-field test shows that intraspinal injection of LV-*Cxcl13* shRNA-2 did not induce sedation. n=7 mice/group. (E, F) Intraspinal injection of LV-*Cxcl13* shRNA-3 attenuated SNL-induced mechanical allodynia (E) and heat hyperalgesia (F). * $P < 0.05$, ** $P < 0.01$. Two–way repeated measures ANOVA followed by Bonferroni test. n=7 mice/group. Arrows indicate lentivirus injection.

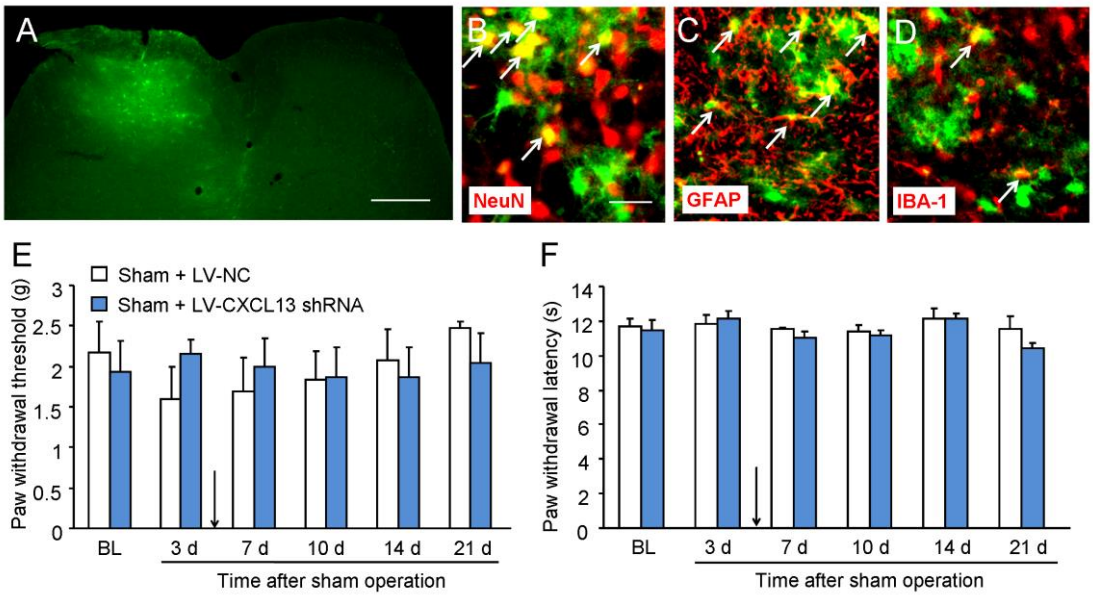

Supplementary Figure 5. The expression of GFP in the spinal cord and the effect of *Cxcl13* shRNA lentivirus on sham-operated animals. (A) Representative fluorescence photomicrograph showing GFP expression in the spinal cord 4 days after intraspinal infusion of lentivirus vector. Scale bar, 200 μm. (B-D) The staining of NeuN, GFAP, and IBA-1 on spinal sections expressing GFP (arrows, double labelled cells). Scale bar, 20 μm. (E-F) Sham operation did not change paw withdrawal threshold (E) or paw withdrawal latency (F) 3 days after surgery. LV-CXCL13 shRNA injection had no effect on threshold or latency (arrows, lentivirus injection). n=5 mice/group.

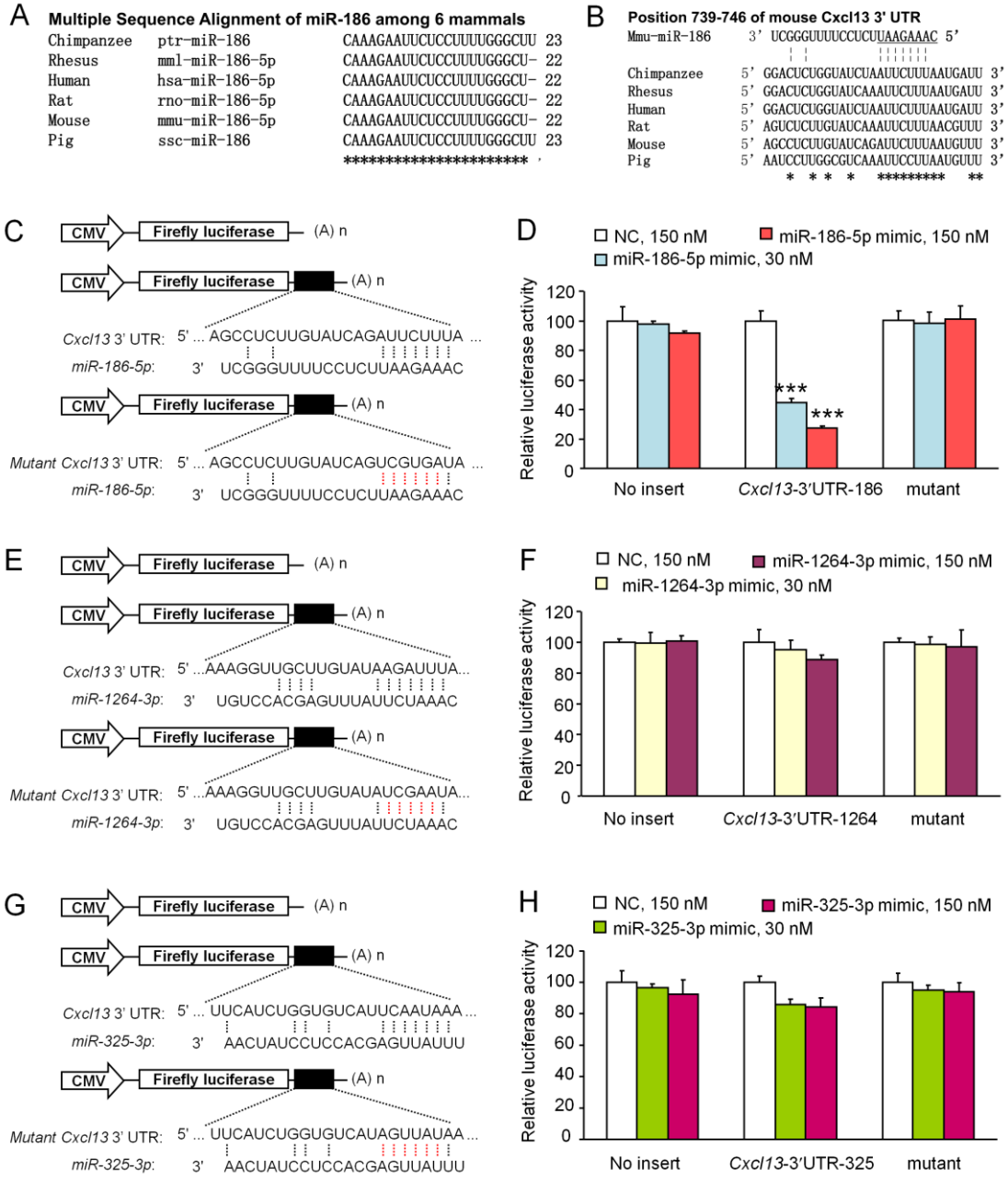

Supplementary Figure 6. miR-186-5p directly targets *Cxcl13* 3′-UTR. (A) Sequences alignment of mmu-miR-186-5p. Mature sequences of miR-186-5p were highly conserved among mammals. Asterisks indicate identical nucleotides. (B) The binding site of miR-186-5p within *Cxcl13* 3′-UTR. The seed sequence is signaled by bold underline. (C) Schematic representations of Cytomegalovirus luciferase constructs used for miR-186-5p reporter assays. (D) miR-186-5p mimic dose-dependently decreased the activity of luciferase in HEK293 cells transfected with

Cxcl13 3′-UTR, but not with mutant *Cxcl13* 3′-UTR. *** P < 0.001 vs. NC. One-way ANOVA followed by Bonferroni test. n=4 for each treatment. (E) Schematic representations of Cytomegalovirus luciferase constructs used for miR-1264-3p reporter assays. (F) miR-1264-3p mimic did not affect the activity of luciferase in HEK293 cells transfected with either *Cxcl13* 3′-UTR or mutant *Cxcl13* 3′-UTR. n=3 for each treatment. (G) Schematic representations of Cytomegalovirus luciferase constructs used for miR-325-3p reporter assays. (F) miR-325-3p mimic did not affect the activity of luciferase in HEK293 cells transfected with either *Cxcl13* 3′-UTR or mutant *Cxcl13* 3′-UTR. n=3 for each treatment.

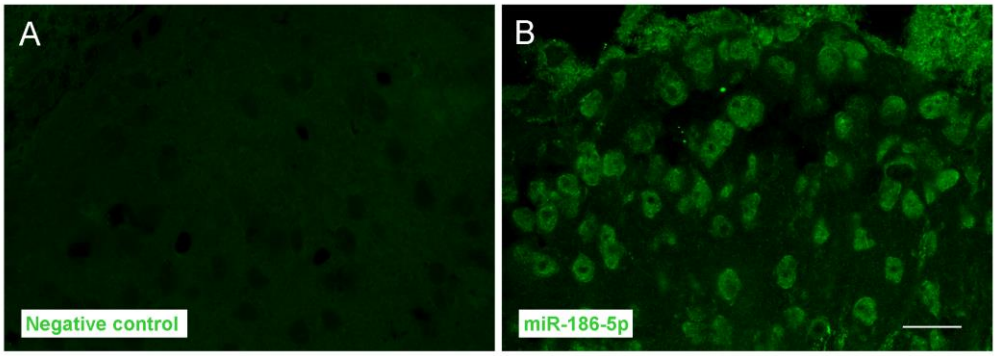

Supplementary Figure 7. Characterization of the specificity of the probe for miR-186-5p. (A) No signal was detected when spinal cord sections were hybridized with the miRCURY LNA™ scramble probe. (B) miR-186-5p was expressed in the spinal cord after incubating the sections with the 5′-DIG and 3′-DIG-labeled mature miRCURY LNA™ detection probe for miR-186-5p. Scale bar, 20 μm.

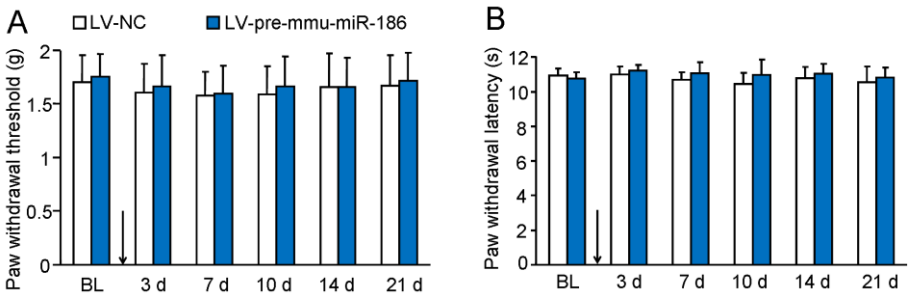

Supplementary Figure 8. Intraspinal injection of LV-pre-mmu-miR-186 in naïve mice did not affect threshold or latency. LV-mmu-miR-186 injection had no effect on paw withdrawal threshold (A) or paw withdrawal latency (B). n=6 mice/group. Arrows, lentivirus injection.

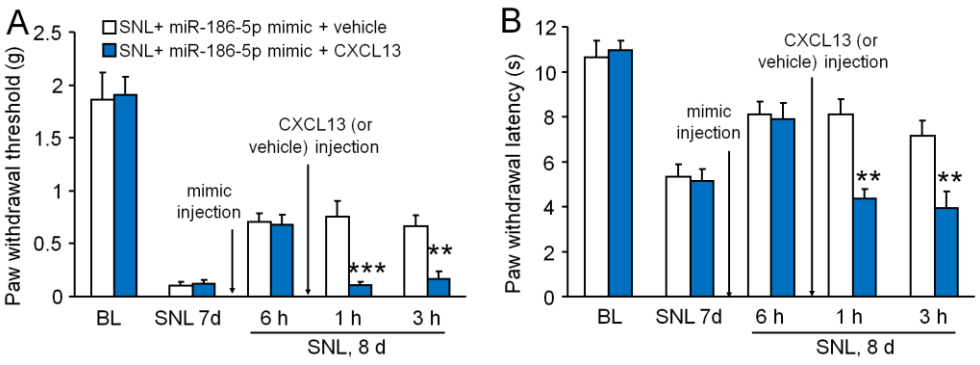

Supplementary Figure 9. Intrathecal CXCL13 reversed the effect of intrathecal miR-186-5p mimic. (A) Intrathecal injection of miR-186-5p mimic attenuated SNL-induced mechancial allodynia 6 h after injection. Further intrathecal injection of CXCL13 (100 ng) reversed the anti-allodynia effect of miR-186-5p mimic. (B) The same treatment of CXCL13 also reversed anti-hyperalgesia effect of miR-186-5p mimic. ** $P < 0.01$, *** $P < 0.001$. Two-way repeated measures ANOVA followed by Bonferroni test. n=5 mice/group.

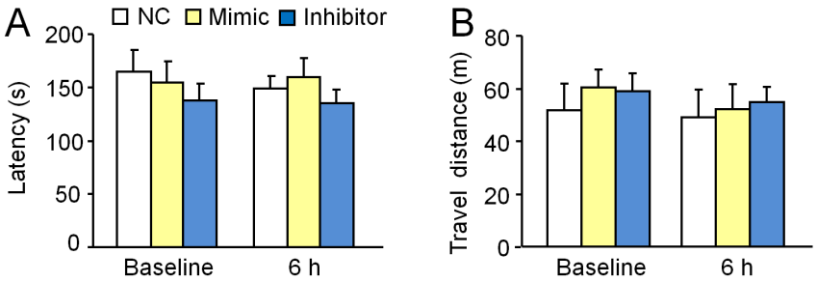

Supplementary Figure 10. The effect of miR-186-5p mimic and inhibitor on motor function and sedation. (A) Rotarod test shows that intrathecal injection of miR-186-5p mimic or inhibitor did not affect motor function of the animals. n=8 mice/group. (B) Open-field test shows that miR-186-5p mimic or inhibitor did not induce sedation. n=9 mice/group.

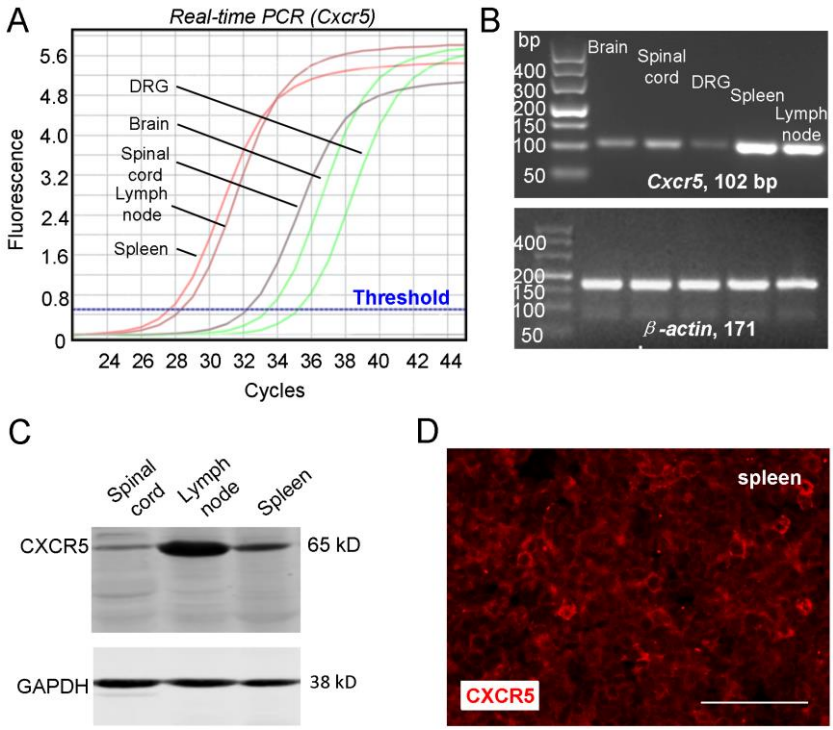

Supplementary Figure 11. CXCR5 expression profile in central nervous system, spleen, and lymph node. (A) Real-time PCR analysis of *Cxcr5* in the brain, spinal cord, DRG, spleen, and lymph node. (B) PCR shows *Cxcr5* expression after 33 cycles of amplification. (C) Western blot shows CXCR5 expression in the spinal cord, lymph node, and spleen in naïve mice. (D) Immunostaining of CXCR5 in the spleen. Scale bar, 50 μm.

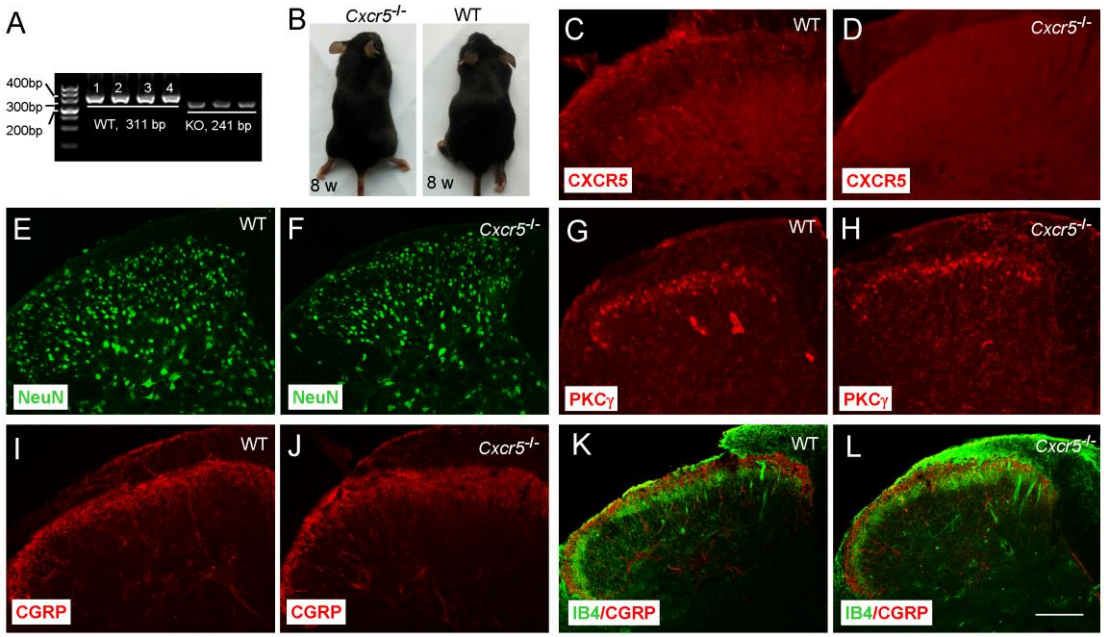

Supplementary Figure 12. Identification of *Cxcr5*$^{-/-}$ mice. (A) PCR-based genotyping of WT and *Cxcr5*$^{-/-}$ mice. (B) Photographs of wildtype (WT, C57BL/6) and *Cxcr5*$^{-/-}$ mice show no changes in gross anatomy of the *Cxcr5*$^{-/-}$ mice. (C, D) Immunostaining shows that CXCR5-IR was shown in WT mice (C) but not in *Cxcr5*$^{-/-}$ mice (D). (E-L) *Cxcr5*$^{-/-}$ mice show normal distribution patterns in the spinal dorsal horn of the neurochemical markers NeuN (F) and PKCγ (H) and normal innervations of the primary afferents labeled with CGRP (J, L) and IB4 (L). CGRP^{+} peptidergic (red) and IB4^{+} non-peptidegic (green) primary afferents are well separated in the superfacial dorsal horn of WT (K) and *Cxcr5*$^{-/-}$ (L) mice. Scale bar, 100 μm.

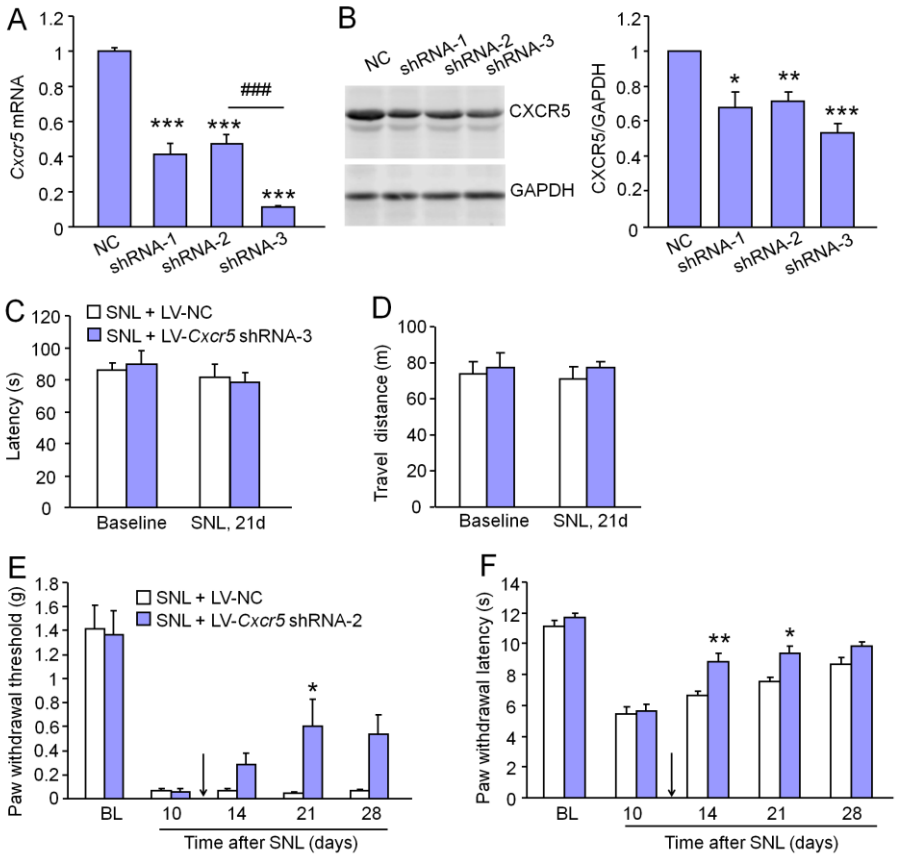

Supplementary Figure 13. Characterization of the knockdown and anti-nociceptive effects of different *Cxcr5* shRNA. (A) Real-time PCR assay of *Cxcr5* shows that all the three shRNAs reduced the *Cxcr5* mRNA expression, and shRNA-3 shows the best knockdown effect. * P < 0.05, *** P < 0.001, compared with NC. Student's *t*-test. n= 6 for each treatment. (B) Western blot shows CXCR5 protein expression after treatment with shRNAs. * P < 0.05, ** P < 0.01, *** P < 0.001, compared with NC. Student's *t*-test. n= 3 for each treatment. (C) Rotarod test shows that intraspinal injection of LV-*Cxcr5* shRNA-3 did not affect motor function of the animals. n=7 mice/group. (D) Open-field test shows that intraspinal injection of LV-*Cxcr5* shRNA-3 did not induce sedation. n=7 mice/group. (E, F) Intraspinal injection of LV-*Cxcr5* shRNA-2 mildly attenuated SNL-induced mechanical allodynia (E) and heat hyperalgesia (F). * P < 0.05, ** P < 0.01. Two–way repeated measures ANOVA followed by Bonferroni test. n=6 mice/group.

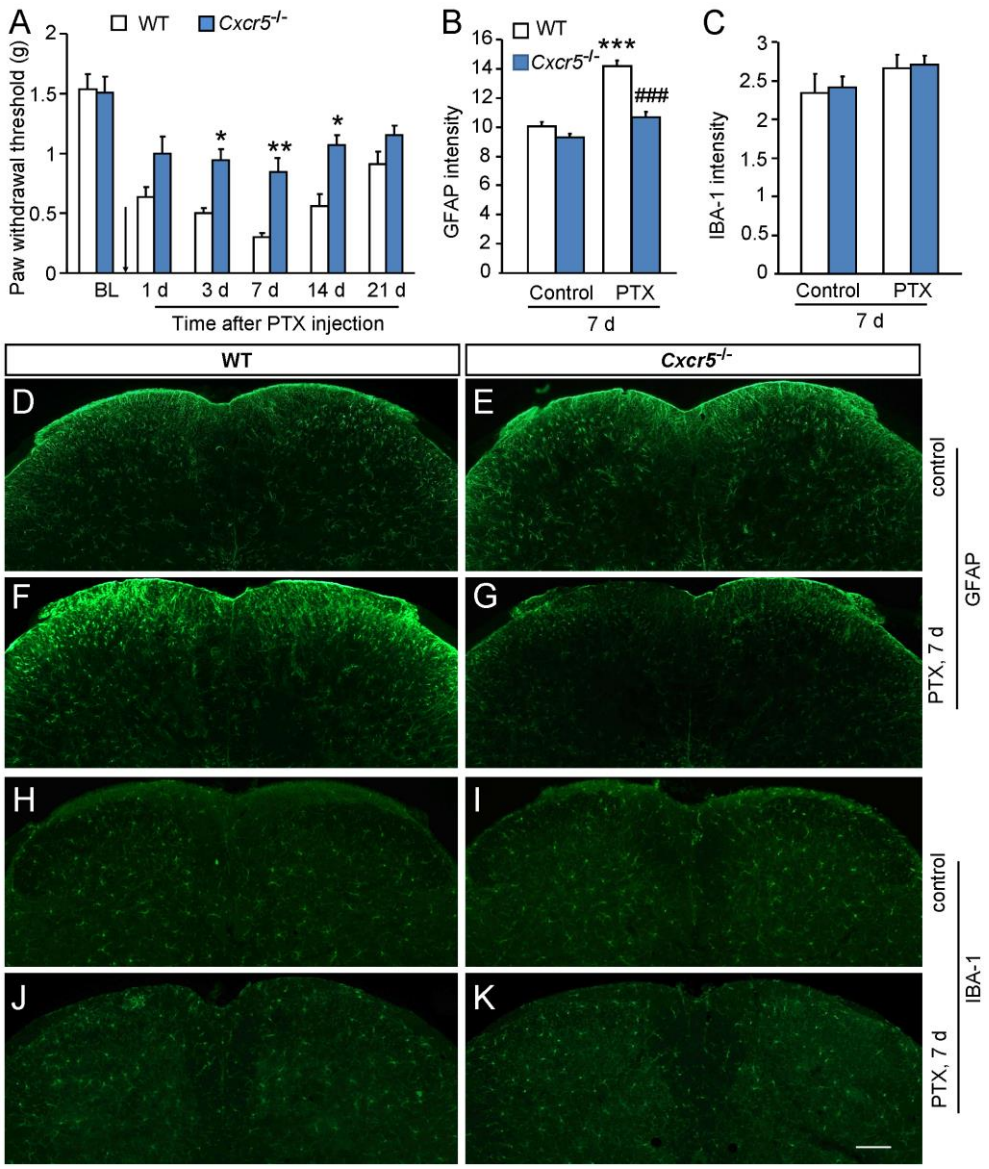

Supplementary Figure 14. Mice lacking *Cxcr5* have defects in chemotherapy pain and astroglial activation. (A) Paclitaxel (PTX)-induced chemotherapy pain was reduced in *Cxcr5*$^{-/-}$ mice from 3 days to 14 days. * P < 0.05, ** P < 0.01, KO vs. WT, two-way repeated measures ANOVA. n=7 mice/group. (B) The intensity of GFAP-IR was increased in WT mice but not in *Cxcr5*$^{-/-}$ mice 7 days after PTX injection. *** P < 0.001, PTX vs. control, ### KO vs. WT. Student's *t*-test. n=3-4 mice/group. (C) The intensity of IBA-1-IR was not changed in either WT or *Cxcr5*$^{-/-}$ mice in the spinal cord at 7 days. n=3-4 mice/group. (D-G) GFAP staining in WT and *Cxcr5*$^{-/-}$ mice. (H-K) IBA-1 staining in WT and *Cxcr5*$^{-/-}$ mice. Scale bar, 200 μm.

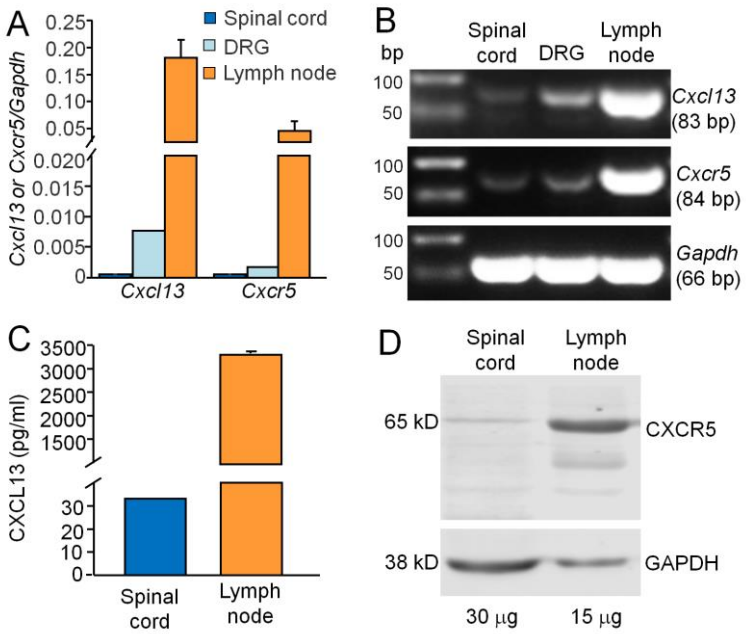

Supplementary Figure 15. CXCL13 and CXCR5 are expressed in human spinal cord, DRG, and lymph node. (A) Quantitative PCR shows the relative mRNA expression of *Cxcl13* and *Cxcr5* (fold to *Gapdh*) in human spinal cord (n=2), DRG (n=1), and lymph node (n=3). (B) PCR shows the expression of *Cxcl13* and *Cxcr5* after 33 cycles' amplification. (C) Elisa shows that CXCL13 protein was expressed in the spinal cord (n=1), and highly enriched in lymph nodes (n=4). (D) Western blot shows CXCR5 expression in the spinal cord and lymph node (30 μg protein for spinal cord and 15 μg protein for lymph node were loaded).